JGR Biogeosciences

RESEARCH ARTICLE
10.1029/2022JG006865

Key Points:

- Light use efficiency (LUE) dominates the responses of gross primary productivity (GPP)-solar-induced chlorophyll fluorescence (SIF) relationship to sky conditions
- SIF_{yield} shows more sensitivity to sky conditions for forest than croplands
- Variations of SIF, SIF_{yield}, GPP and LUE associated with sky conditions are quantified

Supporting Information:

Supporting Information may be found in the online version of this article.

Correspondence to:

Z. Zhang,
zhaoying_zhang@nju.edu.cn

Citation:

Wu, Y., Zhang, Z., Zhang, X., Wu, L., & Zhang, Y. (2022). How do sky conditions affect the relationships between ground-based solar-induced chlorophyll fluorescence and gross primary productivity across different plant types? *Journal of Geophysical Research: Biogeosciences*, *127*, e2022JG006865. https://doi.org/10.1029/2022JG006865

Received 22 FEB 2022
Accepted 28 NOV 2022

How Do Sky Conditions Affect the Relationships Between Ground-Based Solar-Induced Chlorophyll Fluorescence and Gross Primary Productivity Across Different Plant Types?

Yunfei Wu[1,2], Zhaoying Zhang[1,2,3], Xiaokang Zhang[1,2], Linsheng Wu[1,2], and Yongguang Zhang[1,2,4]

[1]Jiangsu Center for Collaborative Innovation in Geographical Information Resource Development and Application, International Institute for Earth System Sciences, Nanjing University, Nanjing, China, [2]Jiangsu Provincial Key Laboratory of Geographic Information Science and Technology, Key Laboratory for Land Satellite Remote Sensing Applications of Ministry of Natural Resources, School of Geography and Ocean Science, Nanjing University, Nanjing, China, [3]Yuxiu Postdoctoral Institute, Nanjing University, Nanjing, China, [4]International Joint Carbon Neutrality Laboratory, Nanjing University, Nanjing, China

Abstract Solar-induced chlorophyll fluorescence (SIF) has been used as a proxy for gross primary productivity (GPP) estimations. However, knowledge on how links between SIF and GPP across different plant types vary in response to sky conditions remain unclear. Here, we investigated the effects of sky conditions on the GPP-SIF relationship based on continuous measurements of SIF and flux across four different plant types. Our analysis shows that the GPP-SIF links are affected by sky conditions and these linking patterns respond differently across plant types. We propose that the inconsistent responses of SIF and GPP to sky conditions are primarily driven by variations in light use efficiency (LUE = GPP/absorbed photosynthetic active radiation (APAR)). Furthermore, we explore a quantitative variation in LUE and SIF_{yield} (SIF/APAR) separately via a decoupling of clearness index (CI) and photosynthetic active radiation under different sky conditions. LUE is more sensitive to sky conditions for the C_3 plants (Forest, Wheat and Rice) than the C_4 plant (Maize), and SIF_{yield} shows more sensitivity to sky conditions for the forest than croplands. Due to the tight link between CI and other environmental factors, the incorporation of CI into the SIF-based GPP model improves GPP estimates for all C_3 plants at both instantaneous and daily scales. Our study implies that a consideration of sky conditions into the SIF-based GPP model can significantly advance the GPP modeling under all sky conditions.

Plain Language Summary An emission of radiation by chlorophyll under the solar light, known as solar-induced chlorophyll fluorescence (SIF), has been widely used to track ecosystem carbon uptake by plants (gross primary productivity, GPP). However, it remains unclear that how responses of links between SIF and GPP to sky conditions vary across plant types. This study explains the responses of GPP-SIF links to various sky conditions across four plant types based on continuous measurements of in situ SIF and flux (the amount of gases exchanged between land surface and atmosphere). We conclude that light use efficiency (LUE, the efficiency of vegetation converting absorbed light into biochemical energy through photosynthesis) dominates the responses of GPP-SIF links to sky conditions for the C_3 plants (such as forest, rice, and wheat). However, LUE for the C_4 plant (Maize) is less sensitive to sky conditions than the C_3 plants, indicating the negligible effects of sky conditions on GPP-SIF links for the C_4 plant. Furthermore, our study also suggests that the integration of sky conditions can improve the accuracy of SIF-based GPP estimation models.

1. Introduction

Sky conditions are closely related to the fractions of clouds and atmospheric aerosol particles, which affect the compositions of direct and diffuse radiation reaching the land surface. The increases in the amount of cloud cover and aerosol loadings in the sky generally decrease the total incoming radiation (direct + diffuse) but increase the fraction of diffuse radiation. Sky conditions are generally characterized using the clearness index (CI), the ratio of direct to total radiation (Dengel & Grace, 2010; Emmel et al., 2020; Park et al., 2018). The variation of CI is not only related to the amount of direct and diffuse radiation, but also indicative of other coupled microclimatic drivers affecting photosynthesis, such as vapor pressure deficit (VPD) and air temperature (T_a) (Gu et al., 1999; Oliphant et al., 2011; Strada et al., 2015). Understanding the effect of sky conditions on photosynthesis would provide essential insights for improving terrestrial ecosystem photosynthesis modeling.

Terrestrial plants generally utilize direct and diffuse radiation with different photosynthesis rates. The days with amplified diffuse light may increase the whole canopy light use efficiency (LUE) in comparison with the days under clear sky conditions when canopy photosynthesis may be reduced by the light saturation effect. Cloudy and overcast sky conditions are usually accompanied by more diffuse radiation and favorable conditions for photosynthesis, therefore, the potential stresses on the canopy photosynthesis can be largely reduced (Dengel & Grace, 2010; Urban et al., 2012). More importantly, diffuse radiation can penetrate deeper into the canopy and thereby enhance canopy photosynthesis of shaded leaves, which is known as the diffuse fertilization effect (Cheng et al., 2015; Gu et al., 2002; Hemes et al., 2020). The diffuse fertilization effect relies on plant characteristics (e.g., canopy structure and C_3 or C_4 photosynthetic pathway). Plant canopies with a taller height and greater leaf area index (LAI) are benefited more from diffuse radiation (Emmel et al., 2020; Hemes et al., 2020; Niyogi, 2004). The reduction in sunlit canopy productivity will be compensated by the increased productivity of the shaded canopy. Compared with light-saturating C_3 plants, C_4 plants generally accommodate high light conditions (Gowik & Westhoff, 2011; Sage & Zhu, 2011; Sharkey, 2019). Hence, the sensitivity of C_3 photosynthesis to cloudy and overcast sky conditions might be greater than that of C_4 plants (Sinclair et al., 1992).

Recently, solar-induced chlorophyll fluorescence (SIF) has provided mechanistic evidence for indicating photosynthesis or gross primary production (GPP) dynamics (Du et al., 2022; Frankenberg et al., 2011; Guanter et al., 2014; Porcar-Castell et al., 2021; Yang et al., 2015). SIF is an electromagnetic signal in the spectral range of 650–800 nm emitted by chlorophyll-*a* molecules during the process of photosynthesis (Baker, 2008). Energy absorbed by plants in the light reactions is competed for by photochemistry, heat dissipation and fluorescence. SIF is closely linked to electron transport and can be used to calculate the electron transport rate in the light reactions (Gu et al., 2019). Therefore, SIF is a good indicator for estimating GPP (Baker, 2008; Porcar-Castell et al., 2014; Zhang et al., 2018). A large amount of research effort has been devoted to GPP-SIF relationships, mainly concentrating on biochemical properties (Atherton et al., 2017), canopy structures (Romero et al., 2018; Yang et al., 2019; Zhang, Zhang, Porcar-Castell, et al., 2020; Zhang et al., 2021), environmental conditions (Chen et al., 2021; Manish Verma et al., 2017; Wieneke et al., 2016) and sun-target-viewing geometries (Hao et al., 2021; He et al., 2017; Liu et al., 2016; Zhang et al., 2018, Zhang, Zhang, Porcar-Castell, et al., 2020). Only a limited number of studies have shown the effect of sky conditions on relationships between SIF and GPP. For example, several previous studies have found that the slope of the GPP-SIF linear model (SIF is the predictor and GPP is the response variable) is greater on cloudy days than on sunny days (Chen et al., 2020; Li et al., 2020; Yang, Ryu, et al., 2018). Miao et al. (2018) discovered that GPP-SIF relationships exhibited different patterns under cloudy conditions compared with sunny conditions. Meanwhile, environmental variables (such as VPD and T_a) related to the sky conditions also have effects on SIF and GPP (Wang et al., 2021; Williams et al., 2016; Yang, Ryu, et al., 2018). To the best of our knowledge, previous efforts have mainly concentrated on photochemistry relevant parameters such as LUE or GPP. However, a comprehensive study on how fluorescence parameters vary under varying sky conditions among different plant types has scarcely been reported.

Therefore, our objectives were: to investigate the responses of the GPP-SIF relationship to sky conditions across different plant types; and to explore whether the GPP modeling accuracy could be improved after incorporating sky conditions into SIF-based GPP models.

2. Materials and Methods

2.1. SIF and Eddy Covariance Flux Observations

Ground-based far-red SIF and eddy covariance (EC) flux measurements during the growing season (Figure S1 and Table S1 in Supporting Information S1) at four sites were utilized in this study, including one forest site: Harvard Forest, and three cropland sites: Avignon Wheat, Jurong Rice and Shangqiu Maize. Information and data references of the four sites are summarized in Table 1.

We installed an automated ground-based continuous observation system named AS-SpecFOM (Agri-SIF Environmental Technology CO., LTD, Nanjing, China) similar to FluoSpec2 (Yang, Shi, et al., 2018) at site Shangqiu, Henan Province, China, to collect seasonal canopy reflectance and SIF observations, which is concurrent with EC flux measurements (~1 km from the EC tower). The system constituted a QEPRO (Ocean Optics, Dunedin, FL, USA) spectrometer which covers a spectral range of 730–785 nm, with a full width half maximum (FWHM) of 0.17 nm and a signal to noise ratio (SNR) of approximately 1,000, which was used for SIF retrievals. Another

Table 1
Basic Information of Four In Situ Continuous SIF and GPP Measurements

Site	Latitude	Longitude	Vegetation type	Years of data			Reference	Retrieval method
Shangqiu	34.5199°N	115.5916°E	Maize	2017	2018	2019	(Li et al., 2020)	SFM
Jurong	31.8068°N	119.2173°E	Rice	2016	2018		(Zhang, Zhang, Porcar-Castell, et al., 2020)	SFM
Avignon	43.9176°N	2.8796°E	Wheat	2010			(Daumard et al., 2010)	FLD
Harvard	42.538°N	72.171°W	Forest	2013	2014		(Yang et al., 2015)	SFM

Note. SFM = spectral fitting method, FLD = Fraunhofer line depth, SIF = solar-induced chlorophyll fluorescence, GPP = gross primary productivity.

spectrometer in this system is HR2000+ (spectral range of wavelength 350–1,000 nm, FWHM of 1.1 nm, Ocean Optics, USA) which was used for canopy reflectance measurements and for canopy vegetation indices (VIs) derivations. The system with a 25° field of view (FOV) was mounted approximately 10 m above the maize canopy. The mean annual temperature is 13.9°C and the mean precipitation is 708 mm.

Site Jurong, located in Jiangsu Province, China, EC flux measurements were also used to measure CO_2 fluxes and another AS-SpecFOM system with FOV of 25° was placed at 8 m above the ground (~20 m from the EC tower) which also includes two spectrometers: QEPRO (range of wavelength 730–780 nm, FWHM of 0.1 nm, SNR of approximately 1,000), and HR2000+ (range of wavelength 400–1,000 nm, FWHM of 3 nm). The mean annual temperature is 15.2°C and mean annual precipitation is 1,058.8 mm.

Yang et al. (2015) used a spectrometer with a spectral resolution of ~0.13 nm (full width at half maximum, FWHM) between 680 and 775 nm for SIF observation and retrieval (HR2000+). Daumard et al. (2010) and Goulas et al. (2017) used two identical spectrometers (FWHM = 0.4 nm) to simultaneously measure radiance and irradiance in the range from 630 to 815 nm (HR2000+). Details of the measurements for the two other sites can be found in: Yang et al. (2015) for the Harvard Forest site (FluoSpec2) and Daumard et al. (2010) and Goulas et al. (2017) for Avignon Wheat (TriFLEX).

The far-red SIF values were retrieved by the spectral fitting method (SFM) method (Meroni & Colombo, 2006; Meroni et al., 2010) for the Harvard, Shangqiu and Jurong sites. The Fraunhofer line depth (FLD) retrieval method was adopted to extract far-red SIF at site Avignon (Plascyk, 1975; Plascyk & Gabriel, 1975). SFM and FLD are both the most common retrieval methods and have been recognized to be capable of accurately retrieving SIF (Meroni et al., 2009). We believe that the SFM algorithm is relatively stable under different sky conditions (Figure S2 in Supporting Information S1). We used EddyPro software (version 6.1.0, LI-COR, USA) to process the flux data. GPP values were estimated by partitioning the net flux of CO_2 measured by flux tower into GPP and ecosystem respiration after being quality controlled (Reichstein et al., 2005). All SIF and GPP observations from 9 a.m. to 4 p.m. were averaged over half-hour intervals, except at the Harvard site where hourly intervals were used. We also conducted data quality control for SIF (Cogliati et al., 2015), and the data were filtered with following conditions: (a) SZA >60°, (b) maximum digital counts >200,000 or <50,000, (c) SNR <30. After the quality control, we further filtered the outliers by statistical methods.

All of the above SIF systems (AS-SpecFOM, FluoSpec2, TriFLEX) used the same hemispherical-conical configurations for SIF measurements, which allow for comparison across sites. Moreover, the bare fiber obtained down-welling and up-welling radiance sequentially with a similar light path-switching approach (separating one optical path into two paths by combining a "Y-shaped" splitter fiber optic and TTL). The core spectrometers contain QE and HR, whose FWHM and SNR are high enough for SIF retrievals (Li et al., 2020; Yang et al., 2015, Yang, Shi, et al., 2018). The view zenith angle (VZA) of the upwelling sensor was approximately zero for cropland sites but 30° for Harvard Forest site to avoid the tower shade (Yang et al., 2015). We acknowledge that the off-nadir observation at Harvard Forest would affect the SIF retrievals to some extent. However, the small VZA did not show clear effects on the GPP-SIF relationship (Yang et al., 2015).

2.2. Estimation of Canopy LUE and SIF_{yield}

The red edge normalized difference vegetation index (NDRE) was used to calculate the fraction of radiation absorbed by the photosynthetically active green component of vegetation ($fPAR_{green}$) for cropland sites according

to Equation 2 (Gitelson, 2018). NDRE was calculated according to Equation 1 where r750 and r705 represent canopy reflectance at the wavelength of 750 and 705 nm, respectively. LUE and SIF_{yield} at Shangqiu, Jurong and Avignon were calculated according to Equations 3 and 4. Different from the other three sites, Yang et al. (2015) used several quantum sensors (PQS-1, Kipp & Zonen B.V., Delft, Netherlands) to measure incident photosynthetic active radiation (PAR) (PAR_{above}) above the canopy, canopy reflected PAR ($PAR_{reflect}$) and transmitted PAR (PAR_{under}) through the canopy. Absorbed photosynthetic active radiation (APAR) (product of PAR and fPAR) was then calculated according to Equation 5, LUE was then calculated as GPP/APAR and SIF_{yield} was calculated as SIF/APAR. Then fPAR for Harvard Forest site was calculated according to Equation 6.

$$\mathrm{NDRE} = \frac{r750 - r705}{r750 + r705} \tag{1}$$

$$\mathrm{fAPR}_{\mathrm{green}} = 1.2531 \times \mathrm{NDRE} - 0.1035 \tag{2}$$

$$\mathrm{LUE} = \frac{\mathrm{GPP}}{\mathrm{PAR} \times \mathrm{fPAR}_{\mathrm{green}}} \tag{3}$$

$$\mathrm{SIF}_{\mathrm{yield}} = \frac{\mathrm{SIF}}{\mathrm{PAR} \times \mathrm{fPAR}_{\mathrm{green}}} \tag{4}$$

$$\mathrm{APAR} = \mathrm{PAR}_{\mathrm{above}} - \mathrm{PAR}_{\mathrm{under}} - \mathrm{PAR}_{\mathrm{reflect}} \tag{5}$$

$$\mathrm{fPAR} = \frac{\mathrm{APAR}}{\mathrm{PAR}_{\mathrm{above}}} \tag{6}$$

2.3. Calculation of Clearness Index

The CI was calculated according to Equation 7 at all four sites. In our study, CI was calculated based on the measurements of BF5 (sunshine sensor, Delta-T Devices, Cambridge, UK). The diffuse fraction was derived by the ratio of diffuse to total radiation (R_d, R_g) measured by BF5. The diffuse fraction is regarded as a substitute for the result of $1 - \mathrm{CI}$. It is worth noting that a higher CI indicates more clear sky conditions, although the relationship between CI and cloudiness is not linear. In this study, we classified sky conditions into three categories according to Dengel and Grace (2010): sunny sky conditions ($\mathrm{CI} > 0.6$), cloudy sky conditions ($0.3 < \mathrm{CI} \leq 0.6$) and overcast sky conditions ($\mathrm{CI} \leq 0.3$). The extreme overcast time period ($\mathrm{CI} < 0.05$) was excluded from the analysis. Note that during sunrise and sunset, CI could be less than 0.6 due to a long light path even under a clear sky. Since the long light path has the similar effects on radiation as clouds, sunrise and sunset were classified as cloudy or overcast in this study. Under the extremely clear conditions, CI is tightly related to the solar zenith angle (SZA), because the later determines the path length of sunlight and thus the diffuse radiation. However, under the cloudy conditions, the correlation between CI and SZA is weakened because the occurrence of cloud would clearly affect CI but not SZA at diurnal and seasonal scale (Figures S3 and S4 in Supporting Information S1). Therefore, the effects of SZA on CI were not considered in this study. Moreover, the solar-target-viewing geometry effects on SIF due to varying SZA were also not considered because the angular effects are minimal under the cloudy conditions (Rogers et al., 2020).

$$\mathrm{CI} = 1 - R_d / R_g \tag{7}$$

We analyzed the relative changes of LUE, GPP, SIF_{yield}, and SIF from sunny and overcast conditions to cloudy conditions (see Figure 5). Four steps were adopted as below:

Step 1: All data points were grouped into several bins based on PAR (100–200, 200–300,…, 2000–2100 μmol/m^2/s);

Step 2: Data points for each PAR were classified into sunny, cloudy, and overcast conditions according to CI;

Step 3: The difference in the averaged LUE (or GPP, SIF_{yield}, and SIF) between cloudy and sunny (or overcast) conditions were calculated for each PAR bin;

Step 4: The average and standard deviation of differences for all PAR bins were calculated.

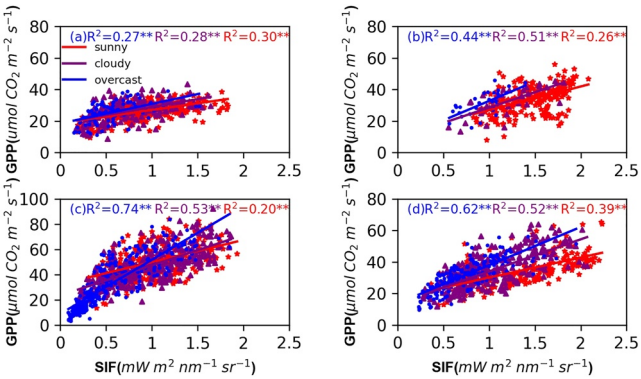

Figure 1. The linear solar-induced chlorophyll fluorescence and gross primary productivity relationships under overcast, cloudy and sunny conditions at (a) Harvard Forest, (b) Avignon Wheat, (c) Shangqiu Maize, and (d) Jurong Rice. R^2 represents the coefficient of determination of fitted linear regressions under different sky conditions. All R^2 values are statistically significant (** for $p < 0.05$).

2.4. Integration of CI Into the SIF-Based GPP Estimation Model

A model integrating CI into the SIF-based GPP model was proposed to mitigate the effect of sky conditions as shown in Equation 8. Here, LUE was represented as a linear transformation of CI (LUE = $a \times \mathrm{CI} + b$) and SIF represented APAR by green vegetation. According to the LUE concept (Monteith, 1972), GPP was expressed as the product of APAR and LUE, and GPP was then determined by the following linear equation:

$$\mathrm{GPP} = A \times \mathrm{SIF} \times (a \times \mathrm{CI} + b) + B \quad (8)$$

where parameters A, B, a, and b represent the slope and intercept of linear fitting optimization. The intercept B was also included here to account for the measurement uncertainties in CI, SIF and GPP.

3. Results

3.1. Relationship Between SIF and GPP Under Different Sky Conditions

Different regression models (linear and hyperbolic) were used to fit GPP-SIF relationships (Table S2 in Supporting Information S1). The differences of R^2 between two fitting models are small under different sky conditions, therefore, we chose the linear model for simplicity purpose. Significant linear relationships were found between instantaneous SIF and GPP at the four sites under different sky conditions (Figure 1). The GPP-SIF relationships varied with the sky conditions, with the highest slope for overcast days and lowest slope for sunny days for all plant types. Meanwhile, the R^2 of GPP-SIF relationships showed the highest values for overcast days and lowest values for sunny days.

We compared PAR with SIF and GPP directly to explore the underlying causes of canopy photosynthesis and fluorescence changes under various sky conditions (Figure 2). We observed a significant positive linear relationship between GPP and PAR under individual sky conditions (Figures 2a–2d). The slope and the goodness-of-fit of linear regression between GPP and PAR tended to be greater when sky conditions changed from sunny to overcast sky conditions. SIF was also positively correlated with PAR (Figures 2e–2h). The variations in the linear

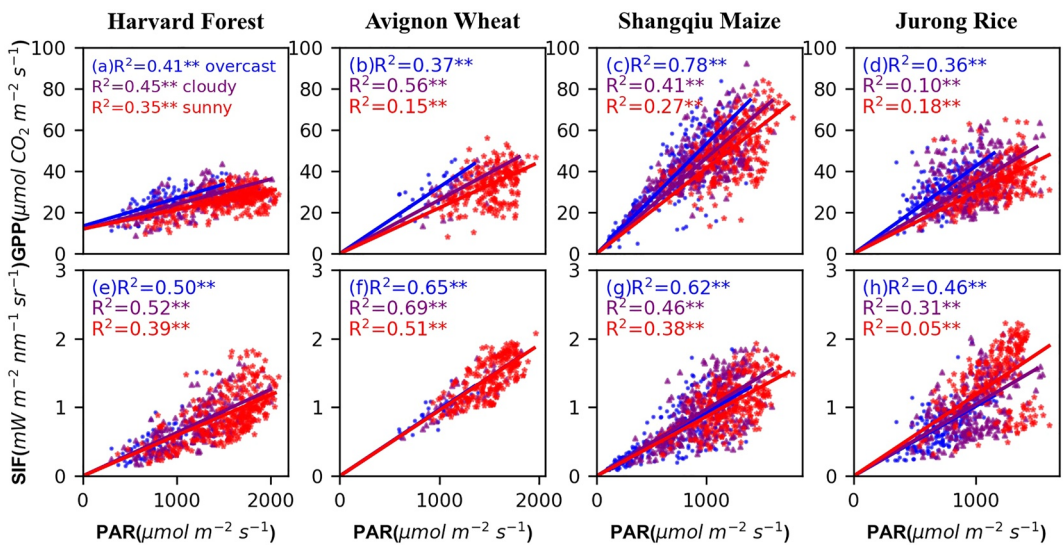

Figure 2. Light response curve of gross primary productivity (GPP) and solar-induced chlorophyll fluorescence (SIF) under overcast, cloudy and sunny conditions at (a) Harvard Forest, (b) Avignon Wheat, (c) Shangqiu Maize and (d) Jurong Rice. Blue, purple and red lines represent the overcast, cloudy and sunny sky conditions, respectively. The R^2 values are the coefficients of determination for the linear relationship between GPP, SIF and photosynthetic active radiation. All R^2 values are statistically significant (** for $p < 0.05$).

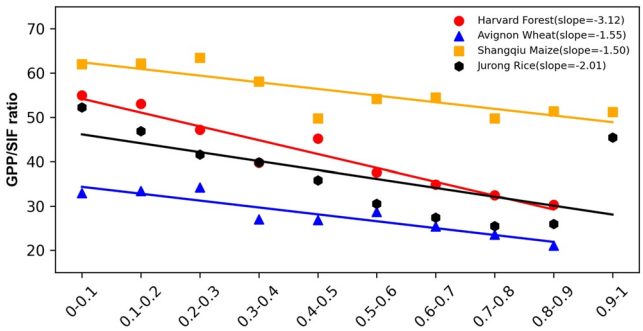

Figure 3. Relationships between clearness index (CI) and gross primary productivity (GPP)/solar-induced chlorophyll fluorescence (SIF) ratio. Instantaneously SIF and GPP were binned into 10 groups based on CI and the mean value of each bin is shown in the figure. The red, blue, yellow, and black lines represent the fitting lines of the linear regression at the Harvard Forest, Avignon Wheat, Shangqiu Maize and Jurong Rice sites, respectively.

regression slopes under all sky conditions were stronger for GPP ~ PAR than for SIF ~ PAR.

To further explore the sensitivity of SIF and GPP links to sky conditions, we compared the GPP/SIF ratio with different levels of CI for the four plant types (Figure 3). We found a clear decreasing trend of GPP/SIF ratio with increasing CI at the four sites and the rate of decrease in the GPP/SIF ratio varied across biomes. The GPP/SIF ratio presented more sensitivities to CI for Forest (slope = −3.12) and Rice (slope = −2.01) than Wheat (slope = −1.55) and Maize (slope = −1.50). Moreover, the GPP/SIF ratio for C_4 plant (maize) was the highest across all CI levels.

3.2. Relationship Between SIF_{yield} and LUE Under Different Sky Conditions

We further investigated the relationships of CI (characteristic of light) or PAR (quantity of light) with LUE and SIF_{yield}. The scattering plots and the correlation coefficients (black numbers) of CI with LUE or SIF_{yield} were presented in Figure 4. In addition, the correlation coefficients (red numbers) of PAR with LUE or SIF_{yield} were also shown for comparison. In particular, the negative correlations would indicate that LUE and SIF_{yield} will increase under the cloudy condition, that is, the LUE or SIF_{yield} enhancements. In general, we observed a statistically significant negative relationship between CI and LUE (Figures 4a–4d), while the relationship between SIF_{yield} and CI was weaker and variable across biomes (Figures 4e–4h). LUE was more sensitive to sky conditions than SIF_{yield} at all four sites. The LUE of C_3 plants showed higher sensitivities to CI than to PAR, while the LUE of C_4 maize plant was more sensitive to PAR than to CI. These results suggested that PAR was a predominant factor controlling the variation of LUE for C_4 plant, while CI was a major contributor for C_3 plant. The partial correlation analysis also led to the same results (Table S3 in Supporting Information S1). Compared with significant enhancements of LUE under cloudy conditions (Figures 4a–4d), no clear SIF_{yield} enhancement was observed at all four sites (Figures 4e–4h).

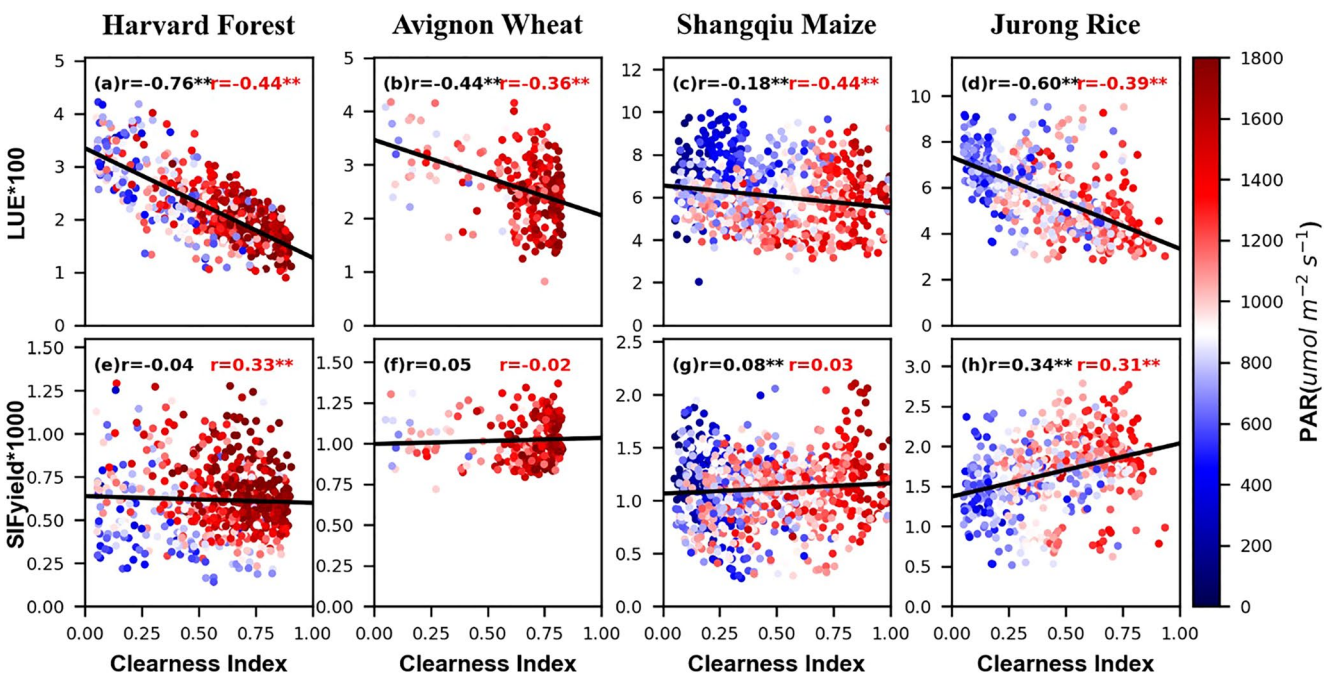

Figure 4. Responses of light use efficiency (LUE) (μmol CO_2/μmol photons) and SIF_{yield} (μmol photons@760 nm/μmol photons) to clearness index (CI) for (a) Harvard Forest, (b) Avignon Wheat, (c) Shangqiu Maize, and (d) Jurong Rice. The correlation coefficients (r) of LUE (or SIF_{yield}) with CI and photosynthetic active radiation were shown in black and in red, respectively. ** denote the statistical significance $p < 0.05$.

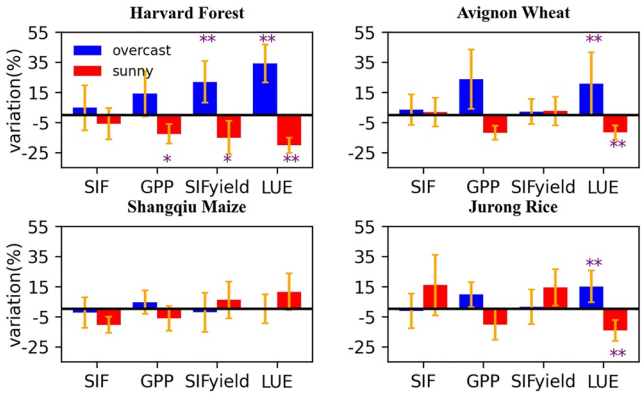

Figure 5. The variations in half-hourly solar-induced chlorophyll fluorescence, gross primary productivity, SIF_{yield} and light use efficiency under overcast or sunny conditions compared with those under cloudy conditions. The black baseline/0-variation value is from cloudy conditions. The orange error bars represent the standard deviation (SD). * and ** denote the statistical significance $p < 0.1$ and 0.05, respectively.

To further quantify the influence of sky conditions on SIF and GPP, we selected cloudy days as a reference to investigate how much SIF_{yield} and LUE varied from cloudy days to overcast days and from cloudy days to sunny days separately by decoupling the covariation of CI and PAR at four sites for the peak growing season (Figure 5). For all C_3 plants, LUE under overcast sky conditions was consistently enhanced to different degrees (Figures 5, 34.17% for Harvard Forest, 20.68% for Avignon Wheat, 14.96% for Jurong Rice) under the same PAR level compared with cloudy sky conditions. Additionally, a reduction in LUE under sunny sky conditions was observed compared with cloudy sky conditions (Figures 5%, −20.17% for Harvard Forest, −11.70% for Avignon Wheat, −14.20% for Jurong Rice). Meanwhile, GPP showed a similar variation trend and variation in magnitude as LUE (Figures 5, 14.11% for Harvard Forest, 23.75% for Avignon Wheat, 9.65% for Jurong Rice enhanced under overcast conditions and −12.67% for Harvard Forest, −11.76% for Avignon Wheat, −10.30% for Jurong Rice decreased under clear conditions). However, for C_4 plant, whether under sunny or overcast sky conditions, the variations in LUE and GPP were much smaller than those for C_3 plants. Different from the large variation in LUE caused by sky conditions, SIF_{yield} showed small variations under overcast conditions at cropland sites, while the variation in SIF_{yield} at the Harvard Forest site reached up to 20% under overcast sky conditions. SIF showed marginal variation in response to sky conditions from cloudy to overcast days for all four sites. Hence, it was elusive for SIF and SIF_{yield} to use a universal model to track the variation in GPP and LUE when sky conditions changed.

3.3. Estimating GPP Based on SIF Under Various Sky Conditions

We further explored how the meteorological factors associated with different sky conditions controlled the GPP-SIF links across different plant types. We compared the relationship between the GPP/SIF ratio and VPD at different levels of air temperature at four sites (Figure 6). The results showed that the GPP/SIF ratio generally decreased with increasing VPD at each air temperature level. In contrast, CI exhibited an opposite trend to the GPP/SIF ratio and increased with the increase in VPD at all sites for each T_a bin (Figure 7). CI increased with increasing VPD, and a significant negative relationship between the GPP/SIF ratio and CI was identifiable across different environmental conditions. Overall, although VPD exerted significant effects on the GPP/SIF ratio, VPD showed a strong coupling relationship with CI, and therefore, CI is representative of the effect of VPD on the relationship between SIF and GPP. Hence, the inclusion of CI alone is expected to achieve improved GPP estimates based on SIF-GPP models.

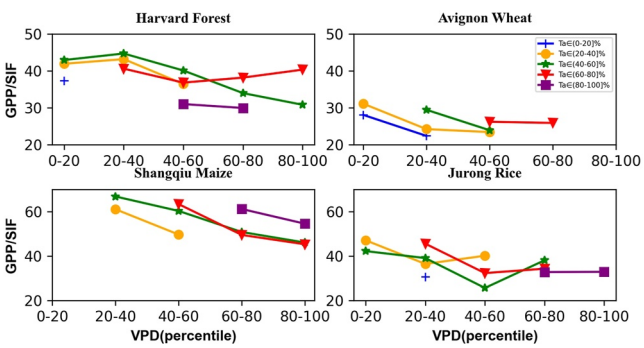

Figure 6. Binned instantaneous gross primary productivity/solar-induced chlorophyll fluorescence ratio over different levels of T_a and vapor pressure deficit values (percentile). Bins with the number of data points less than 10 were filtered.

To further improve the GPP estimate accuracy, we considered the important role of CI in the GPP-SIF relationship, and the performance of GPP modeling from the linear SIF-based GPP model with CI and without CI was compared (Figure 8). It was shown that the integration of CI into the SIF-based GPP model improved the GPP estimation for all C_3 plants at both the instantaneous and daily scales, but not for C_4 plant. The R^2 was improved from 0.42 to 0.52 for rice, from 0.25 to 0.29 for forest and from 0.31 to 0.35 for wheat at the instantaneous scale. The results of daily means also confirmed that the inclusion of CI into the SIF-based GPP model further improved GPP estimation compared with those at the instantaneous scale, with R^2 improving from 0.23 to 0.36 for forest, from 0.22 to 0.25 for wheat and from 0.46 to 0.71 for rice. However, regardless of instantaneous or daily mean data, there was no difference in R^2 before and after including CI in the SIF-based GPP estimation model for maize.

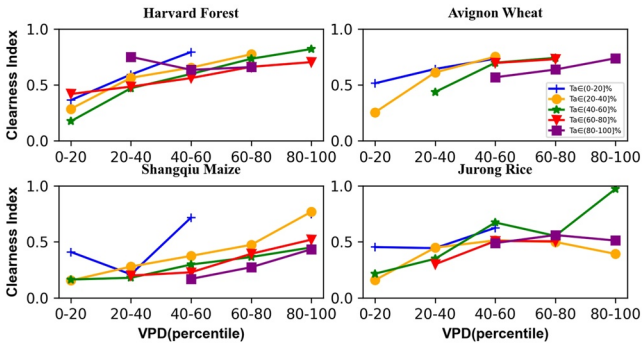

Figure 7. Binned instantaneous clearness index over different levels of T_a and vapor pressure deficit values (percentile).

4. Discussion

4.1. Effect of Sky Conditions on GPP-SIF Relationships

Sky conditions exert significant controls on regulating GPP-SIF relationships across four plant types (Figure 1). CI has been recognized as an indicator to separate clear-sky and cloudy-sky situations and is an important factor controlling the relationship between SIF and GPP on both diurnal and seasonal scales (Figure 1 and Figure S5 in Supporting Information S1). Although previous studies have reported that SIF could be nonlinearly correlated with GPP (Liu et al., 2022) but the linear regression is used to fit the GPP-SIF relationships at all sites mainly because we have classified the data points into three type of sky conditions. SIF under cloudy and overcast conditions is more correlated to (higher R^2) GPP than the model without classifying by sky conditions. We observed that the linear regression between SIF and GPP varied significantly across different sky conditions with the slope and always higher R^2 values under overcast and cloudy situations for all four sites (Figure 1 and Figure S5 in Supporting Information S1).

To explore the mechanisms regarding the major controls on the varying GPP-SIF regression models, we introduce a comparison of PAR with GPP and SIF (Figure 2). The GPP-SIF relationship changes with varying sky conditions due to the divergent responses of GPP and SIF to PAR under various sky conditions. SIF exhibits negligible saturation under high light conditions for neither C_3 nor C_4 plants (Figures 2e–2h); and these findings are consistent with previous studies (Damm et al., 2015; van der Tol et al., 2014). Under overcast and cloudy sky conditions, the linear regression models have steeper slopes between GPP and PAR than under clear sky conditions. Compared with clear sky conditions, plants under overcast/cloudy conditions receive more diffuse light, resulting in an increase in LUE and GPP (Gu et al., 2002; Hemes et al., 2020). However, SIF does not show the same increase under overcast sky conditions as GPP. Hence, SIF is less sensitive to sky conditions than GPP, indicating that GPP dominates in the response of the GPP-SIF relationship to sky conditions. Light saturation of GPP is reduced under heavily diffuse sky conditions (e.g., cloudy and overcast). And hence, SIF is more strongly correlated to GPP under such conditions because neither shows strong light saturation effects. In addition, our results demonstrate that heavily diffuse sky conditions are accompanied with relatively low VPD and temperature in most cases, which have small stresses on plant growth compared with clear sky conditions.

A further investigation of the sensitivity analysis demonstrates that the GPP/SIF ratio tends to decrease with increasing levels of CI for all plant types (Figure 3), which is consistent with studies from Chen et al. (2020), Li et al. (2020) Yang, Ryu, et al. (2018). The GPP/SIF ratio is highest for maize compared with other three plant types, which is primarily attributed to the fact that the photorespiration diminishes the efficiency of photosynthesis for C_3 plants but has little effects on C_4 plant (Gitelson et al., 2018; Wood et al., 2017; Zhang, Zhang, Porcar-Castell, et al., 2020) while SIF is similar for C_3 and C_4 plants under similar environmental conditions. Under high light conditions, oxygen has a high affinity for RuBisCo, increasing photorespiration and reducing photosynthetic efficiency for C_3 plants. However, photorespiration and photosynthetic efficiency is less affected by high light conditions for C_4 plants compared with C_3 plants (Gowik & Westhoff, 2011; Sage & Zhu, 2011). For wheat, the higher SIF due to higher PAR under the cloudy and overcast sky conditions leads to lower GPP/SIF ratio values than forest and rice (Figures 2 and 3). The higher GPP/SIF ratio for forest than rice is mainly because forest is a structurally complex ecosystem with lower SIF escaping probability, and thus lower observed SIF (Zhang, Zhang, Porcar-Castell, et al., 2020). Furthermore, the sensitivity of the GPP-SIF relationship to sky conditions is diverse across ecosystems, and maize and wheat are less sensitive to sky conditions than forest and rice (Figure 3). For maize, the increased carboxylation efficiency and adaptation to high light reduces the sensitivity of GPP to sky conditions compared to light-saturating C_3 species (Gitelson et al., 2018). For wheat,

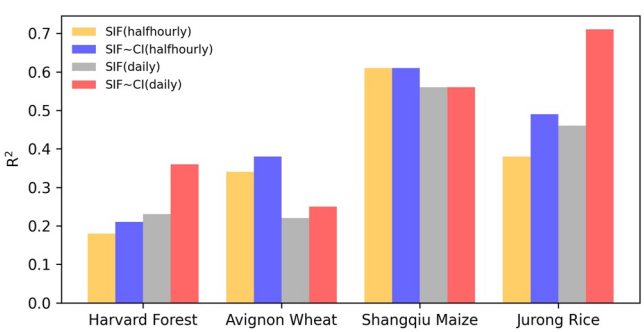

Figure 8. Determination coefficients (R^2) of solar-induced chlorophyll fluorescence-based gross primary productivity estimation models at both half-hour and daily scales with and without considering clearness index.

compared to other C_3 plants (forest and rice), the correlation between CI and GPP/SIF is weaker, which could be caused by the data feature that CI is mainly located in the range of 0.5–0.8 (Figure 4b).

4.2. Response of LUE and SIF_{yield} to Sky Conditions

The effect of sky conditions transitioning from sunny to overcast days mainly leads to a decrease in PAR intensity and a decrease in CI directly which both influence canopy photosynthesis and fluorescence (Dengel & Grace, 2010; Goulas et al., 2017). The GPP/SIF ratio can be simply characterized by LUE/SIF_{yield}, and the variation in the slope of the GPP-SIF relationship is determined by photosynthetic and fluorescence efficiency (Guanter et al., 2014). Our study demonstrates that the mechanisms of the effects of direct and diffuse radiation on canopy photosynthesis are different for C_3 and C_4 plants (Figure 4). CI plays an important role in LUE dynamics for all C_3 plants, while the LUE of maize is more sensitive to PAR (Figure 4b and Table S3 in Supporting Information S1). In contrast, SIF_{yield} is less sensitive to CI or PAR under different sky conditions, which is consistent with previous studies (Goulas et al., 2017). Therefore, the contrasting responses of SIF and GPP to sky conditions are primarily attributed to variations in LUE (Figure 4).

Due to the co-linearity and positive correlations between CI and PAR (Park et al., 2018), as supported in Figure S6 in Supporting Information S1 (All conditions: $r = 0.63$ for Harvard Forest, $r = 0.74$ for Avignon Wheat, $r = 0.65$ for Shangqiu Maize and $r = 0.66$ for Jurong Rice), the influence of CI on GPP-SIF relationships may be partly attributed to the effects of PAR. However, the numerical range of PAR corresponding to the same value of CI is very large. Hence, PAR could not fully explain the variations of CI, which contains information of the diffuse and radiation separately. Therefore, inclusion of CI rather than PAR into GPP-SIF model is necessary under varying sky conditions. After decoupling the influence of CI and PAR (Figure 5 and Table S3 in Supporting Information S1), we find that SIF_{yield} and LUE respond differently to sky conditions among different plant types. The SIF_{yield} enhancement for the forest might benefit from the fact that forest is structurally complex and many layers of shaded leaves photosynthesizing at higher rates under cloudy and overcast days. Moreover, the sensor with viewing zenith angle of 30° at the forest site allows for more observations on shaded leaves below the canopy. However, the SIF_{yield} enhancement is not conspicuous for cropland with simple canopy architecture. The LUE enhancement for C_3 plants under overcast sky conditions is mainly attributed to the more diffuse light that can penetrate deeper into the canopy and be absorbed by light-limited leaves below the canopy according to Figure 5 (Cheng et al., 2015; Emmel et al., 2020; Oliphant et al., 2011). In contrast, LUE for maize is better correlated to PAR than CI (Table S3 in Supporting Information S1) and has negligible light saturation effect; therefore we obtain a weakened diffuse fertilization effect for the LUE for C_4 (Hemes et al., 2020). More importantly, the enhancement magnitude of SIF_{yield} under overcast conditions is only approximately half of the variation in LUE, which implies that SIF_{yield} cannot fully track the variation in LUE caused by sky conditions.

4.3. Integration of CI Into the SIF-Based GPP Estimation Model

A number of studies have reported that favorable conditions (low VPD and preferential temperature) under overcast and cloudy conditions generally enhance canopy photosynthesis (Cheng et al., 2015; Gu et al., 2002; Park et al., 2018). Changes in sky conditions are generally accompanied by varying environmental variables such as VPD and temperature, which possibly alter GPP-SIF relationships (Dengel & Grace, 2010; Paul-Limoges et al., 2018). VPD generally depresses photosynthesis more than fluorescence and hence the GPP/SIF ratio decreases with VPD at all four sites (Figure 6). This demonstrates that the increase in VPD leads to lower stomatal conductance (Strada et al., 2015) and thus GPP, which is mainly responsible for changes of GPP/SIF ratio. However, a high correlation between CI and VPD demonstrates that CI and environmental variables have a synergistic impact on the GPP-SIF links.

By decoupling the effects of PAR and CI, LUE significantly varied as CI changed at C_3 sites (Figure 5). The partial correlation analysis of our study showed that LUE is more correlated with CI at C_3 sites ($\rho = -0.67$ for forest, $\rho = -0.3$ for wheat and $\rho = -0.38$ for rice, $p < 0.05$), while LUE of maize is more related to PAR ($\rho = -0.52$, $p < 0.05$) (Table S3 in Supporting Information S1). From another perspective, the enhancement of LUE under overcast conditions is due to more diffuse radiation, which can be more evenly distributed throughout multilayered canopies (Gu et al., 2003; Knohl & Baldocchi, 2008; Niyogi, 2004). SIF has an advantage in GPP estimation as it contains physiological information about photosynthesis (Porcar-Castell et al., 2014). However,

our results revealed the important role of CI on LUE under different sky conditions for C_3 plants which cannot be tracked by SIF alone. The integration of CI to account for the LUE enhancement under the overcast and cloudy conditions is similar to a previous study at the satellite platform (Zhang, Zhang, Zhang, & Chen, 2020). Therefore, the integration of CI into the SIF-based GPP estimation model is useful when the variation in LUE for C_3 plant is mainly attributed to CI.

Hence, we integrated CI into the SIF-based GPP model, and the GPP modeling accuracy is greatly improved at both the instantaneous and daily scales for C_3 plants. Previous studies also similarly demonstrated that integration of CI or diffuse PAR proportion improves GPP prediction as analyzed by multiple regression analysis (Chen et al., 2020; Yang, Ryu, et al., 2018). The improvements in model performance for forest and rice is greater than 10% at the daily scale, which is clearly higher than the improvement at the diurnal scale (Figure 8). The different improvements between the diurnal and daily scales could be caused by the fact that escape probability (fesc) is nearly constant at the daily scale for the peak growing season but still varies about 10% at the diurnal scale (Figure S7 in Supporting Information S1) (Dechant et al., 2020). This study does not consider fesc because it could not be accurately estimated using the reflectance-based methods.

Furthermore, the improvements at the maize site are very limited since the effect of CI on LUE for C_4 plant is much smaller than that on LUE for C_3 plants. This result is supported by a previous study (Liu et al., 2021) who demonstrated that PAR dominates the variation in LUE rather than CI at the maize site. Due to the weaker sensitivity of C_4 plants to CI than C_3 plants, the weak improvement of integrating CI into the SIF-based GPP estimation model for maize is reasonable. In addition, the weaker improvement in wheat than in forest and rice may be caused by the uneven distribution of CI for wheat, which is consistent with the weak correlation between CI and GPP/SIF (Figure 4b). A separation of photosynthetic pathway is needed when considering the effects of sky conditions on GPP-SIF relationships. Therefore, CI and total radiation should be used for C_3 and C_4 plants respectively when including the sky conditions in the SIF-based GPP estimate model to improve the GPP estimation accuracy in future studies.

5. Conclusions

In this study, we investigated the effects of sky conditions on the GPP-SIF relationship based on ground-based observations at four sites. We found that sky conditions influenced GPP-SIF relationships and that these relationships varied significantly across different plant types. The asynchronous responses of SIF and GPP to sky conditions were primarily depended on the strong sensitivity of LUE to sky conditions. The variations in SIF, SIF_{yield}, GPP, and LUE with sky conditions were quantified by disentangling the effects of CI and PAR. The results suggested that LUE of C_3 plants was more sensitive to CI than that of C_4 plant, whereas SIF_{yield} was more sensitive to sky conditions for forest than croplands. We improved the GPP modeling accuracy by incorporating CI into the SIF-based GPP estimation models for C_3 plants. Our study demonstrates that the consideration of sky condition influences is necessary when scaling SIF to GPP, and can advance the GPP modeling under all sky conditions.

Acknowledgments
This research is financially supported by the National Natural Science Foundation of China (NSFC) for Distinguished Young Scholars (42125105), the Youth Program of NSFC (42101320), and the fellowship of the China Postdoctoral Science Foundation (2021M691491, 2022T150304). We thank Dr. Mark Nearing for scientific writing guidance. We also thank Dr. Qian Zhang and other researchers from Nanjing University for field experiments and data collection. We would also like to acknowledge Xi Yang (geoxiyang@gmail.com) and Yves Goulas (yves.goulas@lmd.polytechnique.fr) for the Harvard Forest and Avignon Wheat flux tower and SIF data. Statistical analysis and visualization of this study were performed using Python 3.6 (Python Software Foundation, USA, https://devguide.python.org/).

Data Availability Statement

The flux tower and SIF time series used in this study can be accessed in https://doi.org/10.6084/m9.figshare.19295009.

References

Atherton, J., Olascoaga, B., Alonso, L., & Porcar-Castell, A. (2017). Spatial variation of leaf optical properties in a Boreal forest is influenced by species and light environment. *Frontiers of Plant Science*, *8*, 309. Original Research. https://doi.org/10.3389/fpls.2017.00309

Baker, N. R. (2008). Chlorophyll fluorescence: A probe of photosynthesis in vivo. *Annual Review of Plant Biology*, *59*(1), 89–113. https://doi.org/10.1146/annurev.arplant.59.032607.092759

Chen, A., Mao, J., Ricciuto, D., Xiao, J., Frankenberg, C., Li, X., et al. (2021). Moisture availability mediates the relationship between terrestrial gross primary production and solar-induced chlorophyll fluorescence: Insights from global-scale variations. *Global Change Biology*, *27*(6), 1144–1156. https://doi.org/10.1111/gcb.15373

Chen, J., Liu, X., Du, S., Ma, Y., & Liu, L. (2020). Integrating SIF and clearness index to improve maize GPP estimation using continuous tower-based observations. *Sensors*, *20*(9), 2493. https://doi.org/10.3390/s20092493

Cheng, S. J., Bohrer, G., Steiner, A. L., Hollinger, D. Y., Suyker, A., Phillips, R. P., & Nadelhoffer, K. J. (2015). Variations in the influence of diffuse light on gross primary productivity in temperate ecosystems. *Agricultural and Forest Meteorology*, *201*, 98–110. https://doi.org/10.1016/j.agrformet.2014.11.002

Cogliati, S., Verhoef, W., Kraft, S., Sabater, N., Alonso, L., Vicent, J., et al. (2015). Retrieval of sun-induced fluorescence using advanced spectral fitting methods. *Remote Sensing of Environment*, *169*, 344–357. https://doi.org/10.1016/j.rse.2015.08.022

Damm, A., Guanter, L., Paul-Limoges, E., van der Tol, C., Hueni, A., Buchmann, N., et al. (2015). Far-red sun-induced chlorophyll fluorescence shows ecosystem-specific relationships to gross primary production: An assessment based on observational and modeling approaches. *Remote Sensing of Environment*, *166*, 91–105. https://doi.org/10.1016/j.rse.2015.06.004

Daumard, F., Champagne, S., Fournier, A., Goulas, Y., Ounis, A., Hanocq, J.-F., & Moya, I. (2010). A field platform for continuous measurement of canopy fluorescence. *IEEE Transactions on Geoscience and Remote Sensing*, *48*(9), 3358–3368. https://doi.org/10.1109/TGRS.2010.2046420

Dechant, B., Ryu, Y., Badgley, G., Zeng, Y., Berry, J. A., Zhang, Y., et al. (2020). Canopy structure explains the relationship between photosynthesis and sun-induced chlorophyll fluorescence in crops. *Remote Sensing of Environment*, *241*, 111733. https://doi.org/10.1016/j.rse.2020.111733

Dengel, S., & Grace, J. (2010). Carbon dioxide exchange and canopy conductance of two coniferous forests under various sky conditions. *Oecologia*, *164*(3), 797–808. https://doi.org/10.1007/s00442-010-1687-0

Du, S., Liu, X., Chen, J., & Liu, L. (2022). Prospects for solar-induced chlorophyll fluorescence remote sensing from the SIFIS payload onboard the TECIS-1 satellite. *Journal of Remote Sensing*, *2022*, 1–9. https://doi.org/10.34133/2022/9845432

Emmel, C., D'Odorico, P., Revill, A., Hortnagl, L., Ammann, C., Buchmann, N., & Eugster, W. (2020). Canopy photosynthesis of six major arable crops is enhanced under diffuse light due to canopy architecture. *Global Change Biology*, *26*(9), 5164–5177. https://doi.org/10.1111/gcb.15226

Frankenberg, C., Fisher, J. B., Worden, J., Badgley, G., Saatchi, S. S., Lee, J.-E., et al. (2011). New global observations of the terrestrial carbon cycle from GOSAT: Patterns of plant fluorescence with gross primary productivity. *Geophysical Research Letters*, *38*(17), L17706. https://doi.org/10.1029/2011gl048738

Gitelson, A. A. (2018). Remote estimation of fraction of radiation absorbed by photosynthetically active vegetation: Generic algorithm for maize and soybean. *Remote Sensing Letters*, *10*(3), 283–291. https://doi.org/10.1080/2150704x.2018.1547445

Gitelson, A. A., Arkebauer, T. J., & Suyker, A. E. (2018). Convergence of daily light use efficiency in irrigated and rainfed C3 and C4 crops. *Remote Sensing of Environment*, *217*, 30–37. https://doi.org/10.1016/j.rse.2018.08.007

Goulas, Y., Fournier, A., Daumard, F., Champagne, S., Ounis, A., Marloie, O., & Moya, I. (2017). Gross primary production of a wheat canopy relates stronger to far red than to red solar-induced chlorophyll fluorescence. *Remote Sensing*, *9*(1), 97. https://doi.org/10.3390/rs9010097

Gowik, U., & Westhoff, P. (2011). The path from C_3 to C_4 photosynthesis. *Plant Physiology*, *155*(1), 56–63. https://doi.org/10.1104/pp.110.165308

Gu, L., Baldocchi, D., Verma, S. B., Black, T. A., Vesala, T., Falge, E. M., & Dowty, P. R. (2002). Advantages of diffuse radiation for terrestrial ecosystem productivity. *Journal of Geophysical Research*, *107*(D6), ACL2-1–ACL2-23. https://doi.org/10.1029/2001jd001242

Gu, L., Baldocchi, D. D., Wofsy, S. C., Munger, J. W., Michalsky, J. J., Urbanski, S. P., & Boden, T. A. (2003). Response of a deciduous forest to the mount Pinatubo eruption: Enhanced photosynthesis. *Science*, *299*(5615), 2035–2038. https://doi.org/10.1126/science.1078366

Gu, L., Fuentes, J. D., Shugart, H. H., Staebler, R. M., & Black, T. A. (1999). Responses of net ecosystem exchanges of carbon dioxide to changes in cloudiness: Results from two North American deciduous forests. *Journal of Geophysical Research*, *104*(D24), 31421–31434. https://doi.org/10.1029/1999jd901068

Gu, L., Han, J., Wood, J. D., Chang, C. Y., & Sun, Y. (2019). Sun-induced Chl fluorescence and its importance for biophysical modeling of photosynthesis based on light reactions. *New Phytologist*, *223*(3), 1179–1191. https://doi.org/10.1111/nph.15796

Guanter, L., Zhang, Y., Jung, M., Joiner, J., Voigt, M., Berry, J. A., et al. (2014). Global and time-resolved monitoring of crop photosynthesis with chlorophyll fluorescence. *Proceedings of the National Academy of Sciences*, *111*(14), E1327–E1333. https://doi.org/10.1073/pnas.1320008111

Hao, D., Asrar, G. R., Zeng, Y., Yang, X., Li, X., Xiao, J., et al. (2021). Potential of hotspot solar-induced chlorophyll fluorescence for better tracking terrestrial photosynthesis. *Global Change Biology*, *27*(10), 2144–2158. https://doi.org/10.1111/gcb.15554

He, L., Chen, J. M., Liu, J., Mo, G., & Joiner, J. (2017). Angular normalization of GOME-2 Sun-induced chlorophyll fluorescence observation as a better proxy of vegetation productivity. *Geophysical Research Letters*, *44*(11), 5691–5699. https://doi.org/10.1002/2017gl073708

Hemes, K. S., Verfaillie, J., & Baldocchi, D. D. (2020). Wildfire-Smoke aerosols lead to increased light use efficiency among agricultural and restored wetland land uses in California's central valley. *Journal of Geophysical Research: Biogeosciences*, *125*(2), e2019JG005380. https://doi.org/10.1029/2019jg005380

Knohl, A., & Baldocchi, D. D. (2008). Effects of diffuse radiation on canopy gas exchange processes in a forest ecosystem. *Journal of Geophysical Research*, *113*(G2), G02023. https://doi.org/10.1029/2007jg000663

Li, Z., Zhang, Q., Li, J., Yang, X., Wu, Y., Zhang, Z., et al. (2020). Solar-induced chlorophyll fluorescence and its link to canopy photosynthesis in maize from continuous ground measurements. *Remote Sensing of Environment*, *236*, 111420. https://doi.org/10.1016/j.rse.2019.111420

Liu, L., Liu, X., Wang, Z., & Zhang, B. (2016). Measurement and analysis of bidirectional SIF emissions in wheat canopies. *IEEE Transactions on Geoscience and Remote Sensing*, *54*(5), 2640–2651. https://doi.org/10.1109/tgrs.2015.2504089

Liu, X., Liu, Z., Liu, L., Lu, X., Chen, J., Du, S., & Zou, C. (2021). Modelling the influence of incident radiation on the SIF-based GPP estimation for maize. *Agricultural and Forest Meteorology*, *307*, 108522. https://doi.org/10.1016/j.agrformet.2021.108522

Liu, Y., Chen, J. M., He, L., Zhang, Z., Wang, R., Rogers, C., et al. (2022). Non-linearity between gross primary productivity and far-red solar-induced chlorophyll fluorescence emitted from canopies of major biomes. *Remote Sensing of Environment*, *271*, 112896. https://doi.org/10.1016/j.rse.2022.112896

Manish Verma, D. S., Evans, B., Frankenberg, C., Beringer, J., Darren, T., Drewry, T. M., et al. (2017). Effect of environmental conditions on the relationship between solar-induced fluorescence and gross primary productivity at an OzFlux grassland site. *Journal of Geophysical Research: Biogeosciences*, *122*(3), 716–733. https://doi.org/10.1002/2016JG003580

Meroni, M., Busetto, L., Colombo, R., Guanter, L., Moreno, J., & Verhoef, W. (2010). Performance of spectral fitting methods for vegetation fluorescence quantification. *Remote Sensing of Environment*, *114*(2), 363–374. https://doi.org/10.1016/j.rse.2009.09.010

Meroni, M., & Colombo, R. (2006). Leaf level detection of solar induced chlorophyll fluorescence by means of a subnanometer resolution spectroradiometer. *Remote Sensing of Environment*, *103*(4), 438–448. https://doi.org/10.1016/j.rse.2006.03.016

Meroni, M., Rossini, M., Guanter, L., Alonso, L., Rascher, U., Colombo, R., & Moreno, J. (2009). Remote sensing of solar-induced chlorophyll fluorescence: Review of methods and applications. *Remote Sensing of Environment*, *113*(10), 2037–2051. https://doi.org/10.1016/j.rse.2009.05.003

Miao, G., Guan, K., Yang, X., Bernacchi, C. J., Berry, J. A., DeLucia, E. H., et al. (2018). Sun-induced chlorophyll fluorescence, photosynthesis, and light use efficiency of a soybean field from seasonally continuous measurements. *Journal of Geophysical Research: Biogeosciences*, *123*(2), 610–623. https://doi.org/10.1002/2017jg004180

Monteith, J. L. (1972). Solar radiation and productivity in tropical ecosystems. *Journal of Applied Ecology*, *9*(3), 747. https://doi.org/10.2307/2401901

Niyogi, D. (2004). Direct observations of the effects of aerosol loading on net ecosystem CO_2 exchanges over different landscapes. *Geophysical Research Letters*, *31*(20), L20506. https://doi.org/10.1029/2004gl020915

Oliphant, A. J., Dragoni, D., Deng, B., Grimmond, C. S. B., Schmid, H. P., & Scott, S. L. (2011). The role of sky conditions on gross primary production in a mixed deciduous forest. *Agricultural and Forest Meteorology*, *151*(7), 781–791. https://doi.org/10.1016/j.agrformet.2011.01.005

Park, S.-B., Knohl, A., Lucas-Moffat, A. M., Migliavacca, M., Gerbig, C., Vesala, T., et al. (2018). Strong radiative effect induced by clouds and smoke on forest net ecosystem productivity in central Siberia. *Agricultural and Forest Meteorology*, *250–251*, 376–387. https://doi.org/10.1016/j.agrformet.2017.09.009

Paul-Limoges, E., Damm, A., Hueni, A., Liebisch, F., Eugster, W., Schaepman, M. E., & Buchmann, N. (2018). Effect of environmental conditions on sun-induced fluorescence in a mixed forest and a cropland. *Remote Sensing of Environment*, *219*, 310–323. https://doi.org/10.1016/j.rse.2018.10.018

Plascyk, J. (1975). The MK II fraunhofer line discriminator (FLD-II) for airborne and orbital remote sensing of solar-stimulated luminescence. *Optical Engineering*, *14*(4), 144339. https://doi.org/10.1117/12.7971842

Plascyk, J. A., & Gabriel, F. C. (1975). The fraunhofer line discriminator MKII-an airborne instrument for Precise and standardized ecological luminescence measurement. *IEEE Transactions on Instrumentation and Measurement*, *24*(4), 306–313. https://doi.org/10.1109/TIM.1975.4314448

Porcar-Castell, A., Malenovsky, Z., Magney, T., Van Wittenberghe, S., Fernandez-Marin, B., Maignan, F., et al. (2021). Chlorophyll a fluorescence illuminates a path connecting plant molecular biology to Earth-system science. *Native Plants*, *7*(8), 998–1009. https://doi.org/10.1038/s41477-021-00980-4

Porcar-Castell, A., Tyystjarvi, E., Atherton, J., van der Tol, C., Flexas, J., Pfundel, E. E., et al. (2014). Linking chlorophyll a fluorescence to photosynthesis for remote sensing applications: Mechanisms and challenges. *Journal of Experimental Botany*, *65*(15), 4065–4095. https://doi.org/10.1093/jxb/eru191

Reichstein, M., Falge, E., Baldocchi, D., Papale, D., Aubinet, M., Berbigier, P., et al. (2005). On the separation of net ecosystem exchange into assimilation and ecosystem respiration: Review and improved algorithm. *Global Change Biology*, *11*(9), 1424–1439. https://doi.org/10.1111/j.1365-2486.2005.001002.x

Rogers, C. A., Chen, J. M., Zheng, T., Croft, H., Gonsamo, A., Luo, X., & Staebler, R. M. (2020). The response of spectral vegetation indices and solar-induced fluorescence to changes in illumination intensity and geometry in the days surrounding the 2017 North American solar eclipse. *Journal of Geophysical Research: Biogeosciences*, *125*(10), e2020JG005774. https://doi.org/10.1029/2020JG005774

Romero, J. M., Cordon, G. B., & Lagorio, M. G. (2018). Modeling re-absorption of fluorescence from the leaf to the canopy level. *Remote Sensing of Environment*, *204*, 138–146. https://doi.org/10.1016/j.rse.2017.10.035

Sage, R. F., & Zhu, X. G. (2011). Exploiting the engine of C_4 photosynthesis. *Journal of Experimental Botany*, *62*(9), 2989–3000. https://doi.org/10.1093/jxb/err179

Sharkey, T. D. (2019). Discovery of the canonical Calvin-Benson cycle. *Photosynthesis Research*, *140*(2), 235–252. https://doi.org/10.1007/s11120-018-0600-2

Sinclair, T. R., Shiraiwa, T., & Hammer, G. L. (1992). Variation in crop radiation-use efficiency with increased diffuse radiation. *Crop Science*, *32*(5), 1281–1284. https://doi.org/10.2135/cropsci1992.0011183X003200050043x

Strada, S., Unger, N., & Yue, X. (2015). Observed aerosol-induced radiative effect on plant productivity in the eastern United States. *Atmospheric Environment*, *122*, 463–476. https://doi.org/10.1016/j.atmosenv.2015.09.051

Urban, O., Klem, K., Ač, A., Havránková, K., Holišová, P., Navrátil, M., et al. (2012). Impact of clear and cloudy sky conditions on the vertical distribution of photosynthetic CO_2 uptake within a spruce canopy. *Functional Ecology*, *26*(1), 46–55. https://doi.org/10.1111/j.1365-2435.2011.01934.x

van der Tol, C., Berry, J. A., Campbell, P. K., & Rascher, U. (2014). Models of fluorescence and photosynthesis for interpreting measurements of solar-induced chlorophyll fluorescence. *Journal of Geophysical Research: Biogeosciences*, *119*(12), 2312–2327. https://doi.org/10.1002/2014JG002713

Wang, X., Wang, C., Wu, J., Miao, G., Chen, M., Chen, S., et al. (2021). Intermediate aerosol loading enhances photosynthetic activity of croplands. *Geophysical Research Letters*, *48*(7). https://doi.org/10.1029/2020GL091893

Wieneke, S., Ahrends, H., Damm, A., Pinto, F., Stadler, A., Rossini, M., & Rascher, U. (2016). Airborne based spectroscopy of red and far-red sun-induced chlorophyll fluorescence: Implications for improved estimates of gross primary productivity. *Remote Sensing of Environment*, *184*, 654–667. https://doi.org/10.1016/j.rse.2016.07.025

Williams, I. N., Riley, W. J., Kueppers, L. M., Biraud, S. C., & Torn, M. S. (2016). Separating the effects of phenology and diffuse radiation on gross primary productivity in winter wheat. *Journal of Geophysical Research: Biogeosciences*, *121*(7), 1903–1915. https://doi.org/10.1002/2015jg003317

Wood, J. D., Griffis, T. J., Baker, J. M., Frankenberg, C., Verma, M., & Yuen, K. (2017). Multiscale analyses of solar-induced fluorescence and gross primary production. *Geophysical Research Letters*, *44*(1), 533–541. https://doi.org/10.1002/2016gl070775

Yang, K., Ryu, Y., Dechant, B., Berry, J. A., Hwang, Y., Jiang, C., et al. (2018). Sun-induced chlorophyll fluorescence is more strongly related to absorbed light than to photosynthesis at half-hourly resolution in a rice paddy. *Remote Sensing of Environment*, *216*, 658–673. https://doi.org/10.1016/j.rse.2018.07.008

Yang, P., van der Tol, C., Verhoef, W., Damm, A., Schickling, A., Kraska, T., et al. (2019). Using reflectance to explain vegetation biochemical and structural effects on sun-induced chlorophyll fluorescence. *Remote Sensing of Environment*, *231*, 110996. https://doi.org/10.1016/j.rse.2018.11.039

Yang, X., Shi, H., Stovall, A., Guan, K., Miao, G., Zhang, Y., et al. (2018). FluoSpec 2—An automated field spectroscopy system to monitor canopy solar-induced fluorescence. *Sensors*, *18*(7), 2063. https://doi.org/10.3390/s18072063

Yang, X., Tang, J. W., Mustard, J. F., Lee, J. E., Rossini, M., Joiner, J., et al. (2015). Solar-induced chlorophyll fluorescence that correlates with canopy photosynthesis on diurnal and seasonal scales in a temperate deciduous forest. *Geophysical Research Letters*, *42*(8), 2977–2987. https://doi.org/10.1002/2015gl063201

Zhang, Z., Zhang, Y., Chen, J. M., Ju, W., Migliavacca, M., & El-Madany, T. S. (2021). Sensitivity of estimated total canopy SIF emission to remotely sensed LAI and BRDF products. *Journal of Remote Sensing*, *2021*, 1–18. https://doi.org/10.34133/2021/9795837

Zhang, Z., Zhang, Y., Joiner, J., & Migliavacca, M. (2018). Angle matters: Bidirectional effects impact the slope of relationship between gross primary productivity and sun-induced chlorophyll fluorescence from Orbiting Carbon Observatory-2 across biomes. *Global Change Biology*, *24*(11), 5017–5020. https://doi.org/10.1111/gcb.14427

Zhang, Z., Zhang, Y., Porcar-Castell, A., Joiner, J., Guanter, L., Yang, X., et al. (2020). Reduction of structural impacts and distinction of photosynthetic pathways in a global estimation of GPP from space-borne solar-induced chlorophyll fluorescence. *Remote Sensing of Environment*, *240*, 111722. https://doi.org/10.1016/j.rse.2020.111722

Zhang, Z., Zhang, Y., Zhang, Y., & Chen, J. M. (2020). Correcting clear-sky bias in gross primary production modeling from satellite solar-induced chlorophyll fluorescence data. *Journal of Geophysical Research: Biogeosciences*, *125*(9), e2020JG005822. https://doi.org/10.1029/2020jg005822